Wu *et al. Chem Synth* 2023;3:39
DOI: 10.20517/cs.2023.20

Chemical Synthesis

Review

Open Access

Check for updates

Mechanisms of nickel-catalyzed reductive cross-coupling reactions

Hongli Wu[1], Shuo-Qing Zhang[1,*], Xin Hong[1,2,3,*]

[1]Center of Chemistry for Frontier Technologies, Department of Chemistry, State Key Laboratory of Clean Energy Utilization, Zhejiang University, Hangzhou 310058, Zhejiang, China.
[2]Beijing National Laboratory for Molecular Sciences, Beijing 100190, China.
[3]State Key Laboratory of Physical Chemistry of Solid Surfaces, Xiamen University, Xiamen 361005, Fujian, China.

[*]**Correspondence to:** Dr. Shuo-Qing Zhang, Center of Chemistry for Frontier Technologies, Department of Chemistry, State Key Laboratory of Clean Energy Utilization, Zhejiang University, 866 Yuhangtang Road, Hangzhou 310058, Zhejiang, China. E-mail: angellasty@zju.edu.cn; Dr. Xin Hong, Center of Chemistry for Frontier Technologies, Department of Chemistry, State Key Laboratory of Clean Energy Utilization, Zhejiang University, 866 Yuhangtang Road, Hangzhou 310058, Zhejiang, China. E-mail: hxchem@zju.edu.cn

How to cite this article: Wu H, Zhang SQ, Hong X. Mechanisms of nickel-catalyzed reductive cross-coupling reactions. *Chem Synth* 2023;3:39. https://dx.doi.org/10.20517/cs.2023.20

Received: 14 Apr 2023 **First Decision:** 19 Jul 2023 **Revised:** 1 Aug 2023 **Accepted:** 25 Aug 2023 **Published:** 20 Sep 2023

Academic Editor: Ying Wan **Copy Editor:** Dan Zhang **Production Editor:** Dan Zhang

Abstract

Nickel-catalyzed reductive cross-coupling (RCC) reactions using two carbon electrophiles as coupling partners provide one of the most reliable and straightforward protocols for facile construction of valuable C-C bonds in the realm of organic chemistry. In recent years, significant progress has been made in the methodological developments and mechanistic studies of these reactions. This review summarizes four widely accepted mechanisms for RCC reactions that have been proposed by experiments or density functional theory calculations. The major difference between these four types of mechanisms lies in the oxidation state of the active catalyst, the change in the valence of nickel during the catalytic cycle, the involvement of carbon radicals, and the form in which the radicals are present. Herein, we focus on covering representative advancements in experimental and theoretical mechanistic studies, aiming to offer vital mechanistic insights into key intermediates, reaction rates, the activation modes of electrophiles, rate- or selectivity-determining steps, and the origin of the cross-selectivity.

Keywords: Mechanisms, nickel catalysis, reductive cross-coupling, C-C bond formation, carbon radicals

INTRODUCTION

Nickel-catalyzed RCC reaction, also known as cross-electrophile coupling (XEC), offers a powerful strategy for C–C bond formation, which has attracted considerable research interest[1-8]. This protocol selectively joins two commercially available electrophiles under reducing conditions with a wide substrate scope of both coupling partners [Scheme 1A and B]. Typically, bidentate and tridentate nitrogen ligands, such as bipyridine (bpy), bioxazoline (biOx), biimidazole (biIm), bisoxazoline (box), terpyridine (terpy), and pyridine-biscarboxamidine (PyBCam), and bidentate phosphine ligands, such as Xantphos, BINAP, and so on, were usually used in this system [Scheme 1C]. In general, when nitrogen ligands are used, the reaction tends to proceed via a radical pathway, while a closed-shell reaction generally occurs with phosphine ligands. There are various mild reducing conditions available, including metal reductants such as Mn and Zn[9,10] and organic reductants such as B_2pin_2 and hydrazine[11,12]. In addition, photoredox catalysis[13-17] and electrochemistry[18-23] can also be utilized [Scheme 1D]. This strategy enables the construction of a range of $C(sp^2)$–$C(sp^2)$[24-26], $C(sp^2)$–$C(sp^3)$[27-31], and $C(sp^3)$–$C(sp^3)$[32-34] bonds with high levels of cross-selectivity and stereoselectivity. For example, Kim *et al.* discovered the first nickel-catalyzed RCC of aryl chlorides with primary alkyl chlorides, utilizing a small amount of iodide or bromide in conjunction with the pyridine-2, 6-bis(N-cyanocarboxamidine) (PyBCamCN) ligand and Zn reductants[28].

With the continuous development of RCC reactions, some mechanistic problems have sparked intense research interest of chemists [Scheme 1E]: (1) The mechanism of RCC deviates from traditional cross-coupling (XC) reactions that typically proceed through oxidative addition (OA)/transmetalation (TM)/reductive elimination (RE) process[35,36]; (2) Nickel intermediates likely possess various oxidation states ranging from Ni^0 to Ni^{IV}; (3) Reaction appears to undergo both two-electron and single-electron redox processes; (4) The radical forms are involved in cage-escaped radicals or solvent caged radicals; (5) The origin of cross-selectivity over homo-selectivity involved in reactions. Until now, considerable achievements have been made in both experimental and computational mechanistic studies to answer these mechanistic problems[37-44]. In this review, we focus primarily on the mechanistic aspects of RCC reactions, with an emphasis on experimental studies, such as stoichiometric, competitive, radical, kinetics, kinetic isotope effect (KIE) experiments, and so on. However, we also take into account theoretical research where appropriate. The aim of this review is to enhance the comprehension of the mechanism and selectivity of these reactions, thereby aiding chemists in designing novel catalytic systems. In the following sections, we will provide an integrated discussion of these mechanisms, including their fundamental steps, catalytic systems, detailed mechanistic studies, and the origin of cross-selectivity.

THE INVESTIGATION OF MECHANISM I

Scheme 2 depicts the scenarios of Mechanism I, which consists of five elementary steps: OA, radical addition, RE, radical formation, and reduction. This mechanism essentially proceeds through a radical chain process and involves a key $Ni^0/Ni^{II}/Ni^{III}$ catalytic cycle. It is worth emphasizing that radicals are generated at one nickel center, and the resulting cage-escaped radicals subsequently combine with another nickel species prior to the OA step. Additionally, when a photoredox catalyst is employed, the formation of radicals may exhibit variability and typically be independent of the catalytic cycle of nickel. A detailed discussion on this will be presented later. Finally, it should be noted that in the product release process, no reducing agents are involved. Alternatively, there is another possibility that radicals may directly combine with Ni^0 to form Ni^I [45,46] intermediates. Xu *et al.* has computationally demonstrated that even though the addition of radicals to Ni^0 is energetically more favorable than the OA of Ni^0 to substrates aryl bromides, OA still occurs due to the low concentration of radicals and the abundance of aryl bromides[47]. Hence, it will not be further elaborated here.

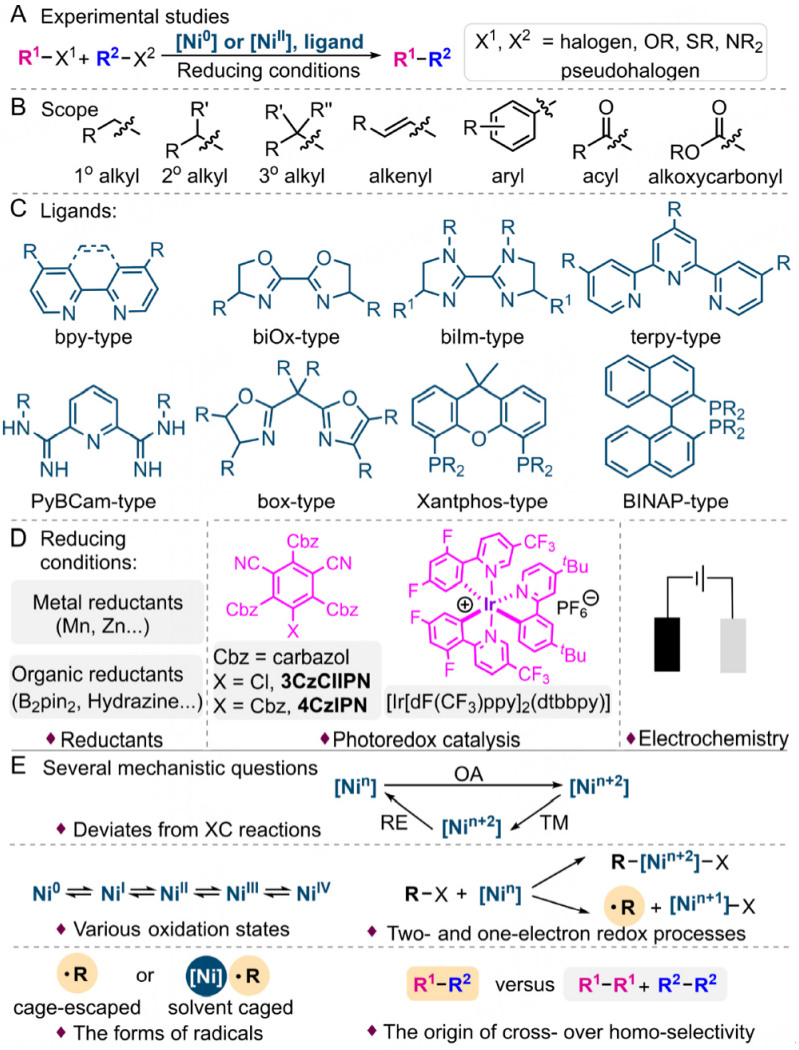

Scheme 1. Nickel-catalyzed reductive cross-coupling reactions. (A) Experimental studies; (B) The scope of substrates; (C) Some common ligands; (D) Reducing conditions; (E) Several mechanistic questions.

Mechanism I predominantly occurs in the Ni^0-catalyzed reductive couplings between $C(sp^2)$ and $C(sp^3)$ electrophiles in the presence of pyridine-type nitrogen ligands and Zn or Mn reductants. The substrates for this mechanism mainly consist of unactivated simple halogenated hydrocarbons. As shown in Figure 1A, Biswas *et al.* conducted a series of experimental mechanistic investigations on the Ni^0/L_1 (L_1 = 4,4'-di-tert-butyl-2,2'-bipyridine (dtbpy))-catalyzed RCC of iodobenzene **1a** with iodooctadecane **1b**, using Mn as a reductant[48]. Compared to the previously published reactions[49,50], several small modifications were made to these reaction conditions.

According to Mechanism I, the reaction begins with the initial OA to give Ni^{II} intermediate. To determine whether aryl or alkyl Ni^{II} intermediate was formed initially, competition reaction studies between **1a** and **2a** were performed [Figure 1B]. The results showed that iodobenzene reacts with Ni^0 species 4.7 times faster than iodooctadecane, which preferentially leads to Ni^{II} aryl intermediate. Wotal *et al.* also isolated Ni^{II} acyl intermediates and discovered that they can react with a series of carbon electrophiles[51]. In addition, the similar aryl nickel complex [(dtbpy)Ni^{II}(*o*-tolyl)I] was synthesized by Sheng *et al.*[52]. Subsequently, stoichiometric experiment studies between isolated and characterized Ni^{II} aryl intermediates **IM1** and **1b**

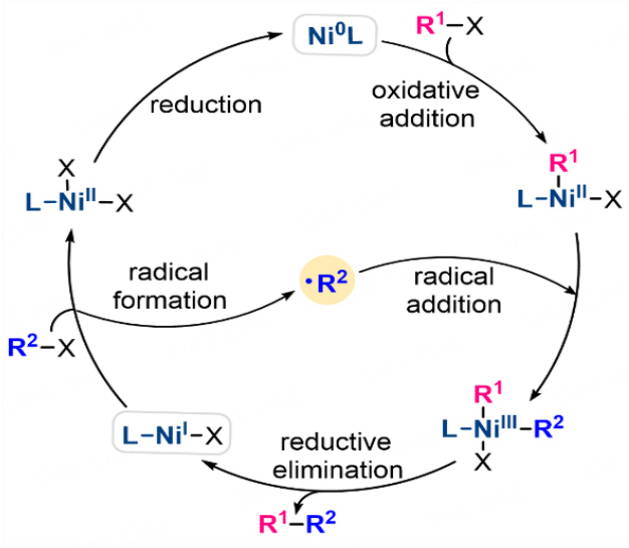

Scheme 2. The catalytic cycle of Mechanism I.

were conducted to further verify that **IM1** acts as the initial key intermediate of the catalytic cycle [Figure 1C]. Significantly, cross-product **4c** can be formed through this process without the Mn reductant, which not only confirms that Ni^{II} aryl species is the active intermediate of the reaction but also proves the release of the product does not require reducing agents. Moreover, radical clock experiments implied that the alkyl radical would be formed in the system [Figure 1D]. Furthermore, the findings from radical lifetime studies reveal a positive linear correlation between the **7c**/**8c** ratio and the catalyst concentration [Ni], suggesting the involvement of a radical chain process [Figure 1E]. Additionally, they carried out organometallic experiments and excluded the possibility of an organozinc reagent acting as an intermediate. Based on all the experimental mechanistic investigations, it has been confirmed that this type of transformation [Figure 1A], which is restricted to the coupling of $C(sp^2)$ electrophiles with $C(sp^3)$ electrophiles, predominantly proceeds through a radical chain pathway.

More importantly, Biswas *et al.* also elucidated the origin of the cross-selectivity over homo-selectivity[48] [Figure 2]. They found that iodobenzene PhI reacts with Ni^0 species faster than iodooctadecane $C_8H_{17}I$ to afford Ni^{II} aryl intermediate, while $L_1Ni^{I}I$ species may react with $C_8H_{17}I$ rather than PhI, resulting in alkyl radicals. This sequential activation mode accounts for the experimentally observed cross-selectivity. Typically, due to the lower stability of aryl radicals compared to alkyl radicals, $C_8H_{17}I$ is more prone to generate radicals by reacting with Ni^0 species. In contrast, PhI is more likely to undergo OA with Ni^0 species, which can be attributed to the favorable π-metal interactions between the substrate and the metal[53]. Several theoretical calculations have confirmed that $C(sp^2)$ electrophiles undergo OA more rapidly than $C(sp^3)$ electrophiles. For instance, Ren *et al.* demonstrated that the activation energy barrier of aryl halides is 4.4 kcal/mol lower than alkyl halides[54]. Similarly, Kumar *et al.* obtained identical results[55].

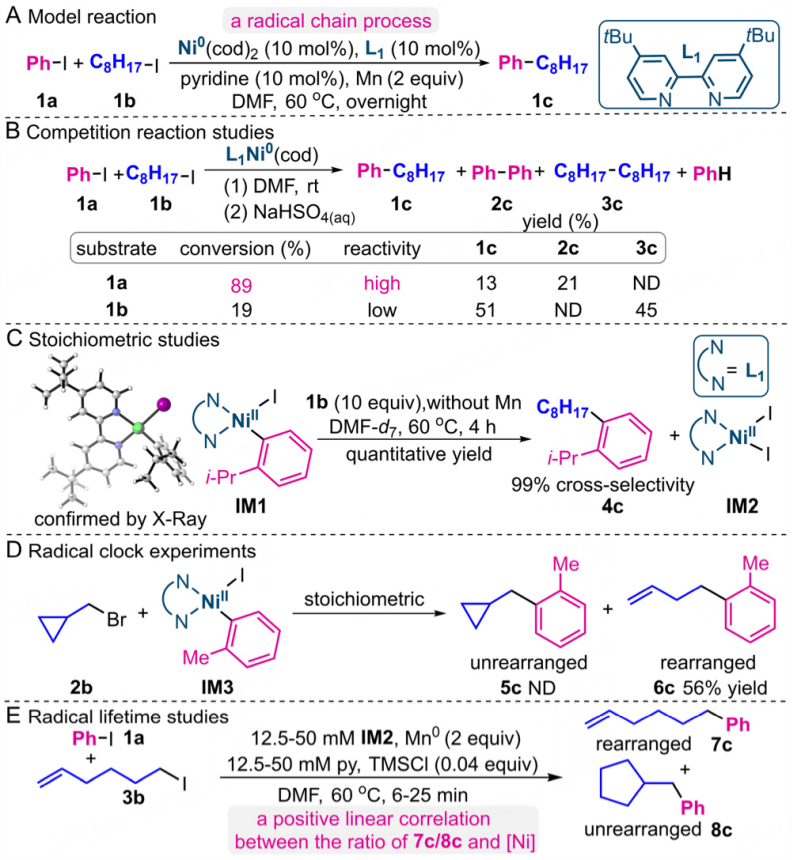

Figure 1. Experimental mechanistic investigations of Mechanism I. (A) Model reaction used in experimental mechanistic investigations; (B) Competition reaction studies between **1a** and **1b**; (C) Stoichiometric studies of **IM1**; (D) Radical clock experiments; (E) Radical lifetime studies. DMA: N,N-Dimethylformamide; TMSCl: Trimethylchlorosilane; ND: not detected; Conversion with respect to the amount of L_1Ni^0(cod).

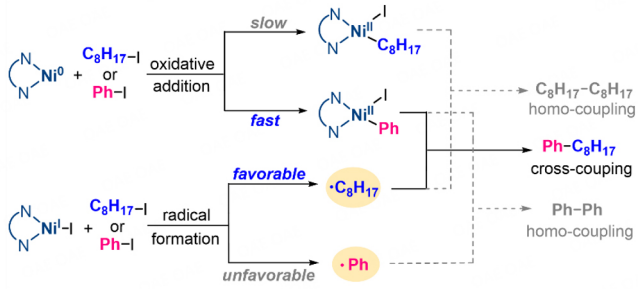

Figure 2. The origin of the cross-selectivity.

It is gratifying to note that Ren *et al.* performed detailed density functional theory (DFT) calculations on $NiBr_2$/4,4'-di-methyl-2,2'-bipyridine-catalyzed RCC of aryl bromide and alkyl bromide[54]. They found that radical addition is the rate-limiting step with the energy barrier of 10.4 kcal/mol, suggesting that the radical chain mechanism is a feasible process. In addition, Wang *et al.* disclosed this mechanism still operates when aryl iodides and tertiary alkyl halides are used[56]. These two research groups also independently calculated an alternative Mechanism II (discussed below), and both mechanisms are energetically feasible, making it difficult to distinguish between them based solely on calculations. Recently, Ji *et al.* carried out experimental

mechanistic investigations on the Ni(1,2-Dimethoxyethane (DME))Br_2/box-catalyzed enantioselective coupling of acid chlorides with α-bromobenzoates, indicating that this system also follows a radical chain mechanism[57]. It is worth noting that some of the recently developed Ni/photoredox[58-62] and Ni/electrochemistry[63,64] dual catalytic RCCs also involve a radical chain process. Despite the changes in reduction conditions, the essence of the Ni-involved catalytic cycle remains unchanged, primarily influencing the formation pathway of the radicals.

Although Weix proposed a possible mechanism and suggested that radicals may be generated with the assistance of $Ni^{I}X$ species, no conclusive evidence has been provided to support this claim. Building on previous studies[65-69], there are four different pathways that can be taken, including single electron transfer, either outer-sphere or inner-sphere, two-electron OA, and concerted halogen-atom abstraction, as shown in Figure 3.

Thankfully, Lin *et al.* used electrochemical methods and DFT calculations to investigate the activation modes of radical formation in the (bpy)Ni-catalyzed system[69]. They ruled out electron transfer and two-electron OA and revealed radical formation occurs through a halogen atom abstraction process via transition state **TS1**, with the energy barrier of 7.4 kcal/mol [Figure 4]. Note that, unlike the study of Weix, the radical is assisted by Ni^{I} aryl intermediates **IM4** rather than $Ni^{I}X$ in this process. Additionally, Diccianni *et al.* further confirmed that alkyl radicals are generated in a similar manner in the (Xantphos)Ni-catalyzed system with the aid of kinetic studies and DFT calculations[65].

Of particular note, photoredox catalysts can also aid in the generation of radicals. In a study by Wang *et al.*, they reported a Ni/photoredox-catalyzed enantioconvergent RCC between α-bromophosphates and aryl iodides[60] [Figure 5A]. To determine whether the radicals were generated by the photoredox catalyst or the nickel, they conducted comparison experiments using substrates **3a** and **5b** under conditions with photoredox and Ni catalysts, respectively [Figure 5B]. The results showed that the photoredox catalyst was responsible for generating the desired product **10c**, suggesting that the radicals are formed by the photoredox catalyst in this system. The process of free radical formation is illustrated in Figure 5C. Initially, the photoredox catalyst 4CzIPN is excited by light, and the resulting excited $4CzIPN^{*}$ subsequently undergoes reductive quenching with Hantzsch ester (HEH), leading to $4CzIPN^{-\bullet}$ with a strong reducing capacity [$4CzIPN/4CzIPN^{-\bullet}$ = -1.21 *vs.* saturated calomel electrode (SCE)]. Eventually, the single-electron transfer process occurs between $4CzIPN^{-\bullet}$ and **5b** to release radicals and regenerate photoredox catalyst 4CzIPN. Moreover, they also confirmed that the radical addition step is the enantioselectivity-determining step through DFT calculations. Similar results were also reported in the work by Guo *et al.* for the Ni/photoredox-catalyzed enantioselective three-component carboarylation of alkenes with tertiary and secondary alkyltrifluoroborates and aryl bromides[70]. It is important to note that the photoredox catalysts assisted generation of radicals occurs independently of the Ni catalyst. Consequently, this catalytic cycle involves a $Ni^{0}/Ni^{II}/Ni^{III}/Ni^{I}/Ni^{0}$ sequence, in which the reduction occurs directly from Ni^{I} to Ni^{0}, rather than the $Ni^{I}\rightarrow Ni^{II}\rightarrow Ni^{0}$ pathway proposed by Weix, where Ni^{I} reacts with alkyl halides to generate radicals and Ni^{II}, followed by the reduction of Ni^{II} to Ni^{0}.

THE INVESTIGATION OF MECHANISM II

As shown in Scheme 3, unlike the radical chain process, Mechanism II proceeds through successive OA, reduction, OA, RE, and reduction, and it features a key $Ni^{0}/Ni^{II}/Ni^{I}/Ni^{III}$ process. Notably, the second OA can occur via a concert two-electron ($Ni^{I}\rightarrow Ni^{III}$, black line) or stepwise single-electron process ($Ni^{I}\rightarrow Ni^{II}\rightarrow Ni^{III}$, blue line). When $C(sp^2)$ electrophiles are used, the reaction generally undergoes a two-electron OA process. On the other hand, the reaction can generate radicals through a single electron process when the

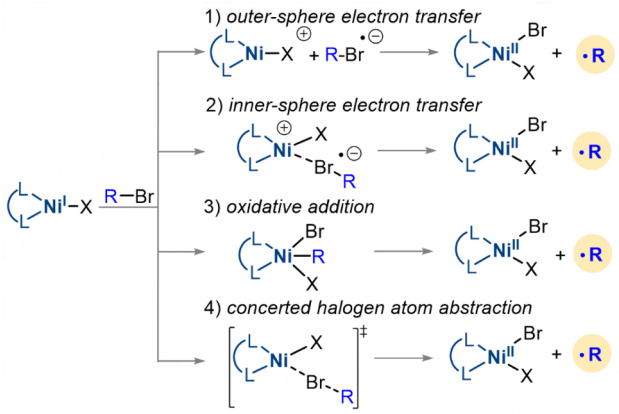

Figure 3. Several pathways for radical formation.

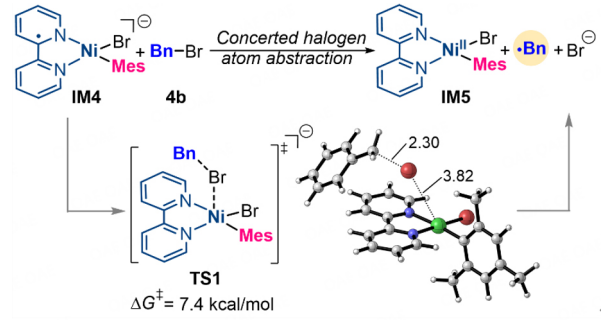

Figure 4. Concerted halogen atom abstraction process. Selected bond distances are given in Å.

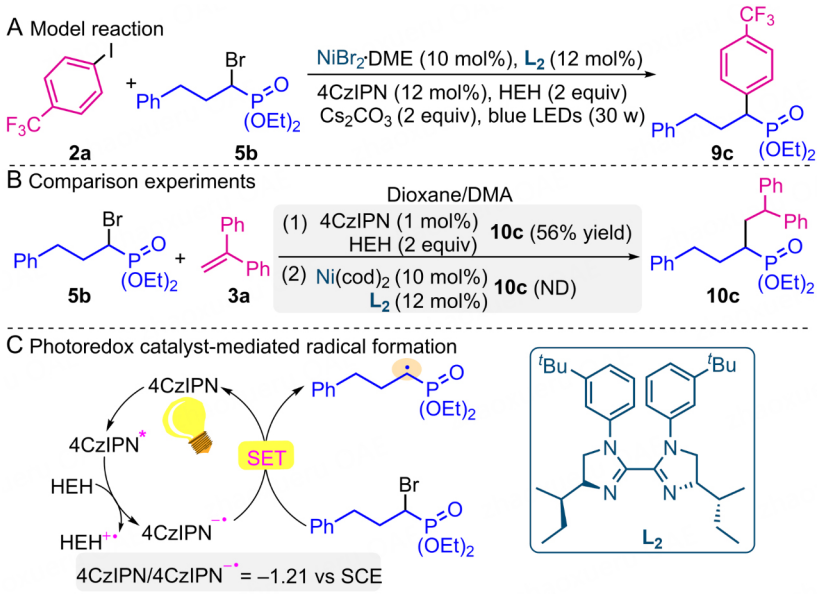

Figure 5. Photocatalyst-assisted radical formation. (A) Model reaction of Ni/photoredox-catalyzed enantioconvergent reductive cross-couplings; (B) Competition experiments between **3a** and **5b**; (C) Photoredox catalyst-mediated radical formation process. SCE: saturated calomel electrode.

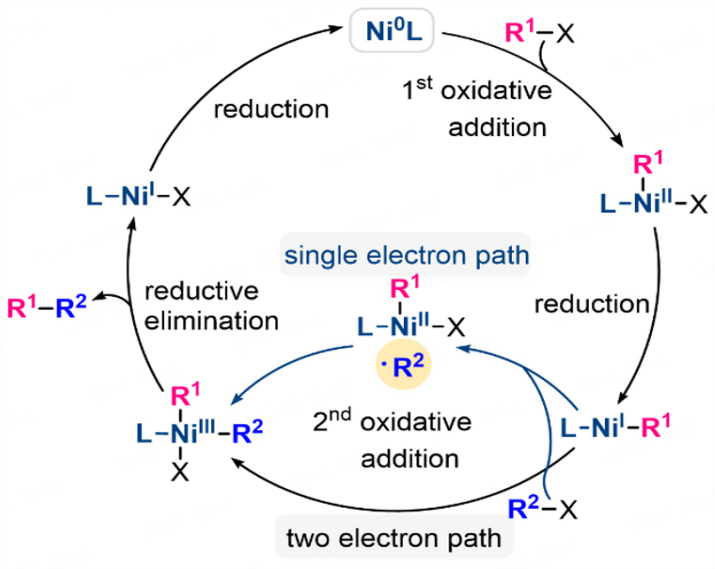

Scheme 3. The catalytic cycle of Mechanism II.

C(sp^3) electrophiles are present. The main differences between Mechanism II and Mechanism I can be summarized as follows: (1) Mechanism II involves twice OA and reduction and requires a reduction step before the release of the product, while Mechanism I only experiences once OA and reduction in the whole catalytic cycle; (2) Mechanism I necessarily involves the radicals, and the formation of radicals occurs prior to OA, whereas Mechanism II may or may not involve radicals. Even if radicals are involved, they are of the solvent-caged type and undergo a radical rebound process during the reaction while being cage-escaped radicals in Mechanism I.

Mechanism II is mainly observed in reductive coupling systems involving C(sp^2)-C(sp^2) electrophiles or C(sp^2)-C(sp^3) electrophiles, which are catalyzed by nickel/pyridine-type ligands in the presence of metal reductants. Generally, when C(sp^3) electrophiles are involved, the system may generate radical intermediates, making it difficult to distinguish from Mechanism I merely from a computational point of view. In such cases, corresponding experimental mechanistic studies are needed to differentiate between them. As early as 2014, Jiang *et al.* investigated the mechanisms on (dtbpy)Ni/Zn-catalyzed RCC reaction of aryl halides from a theoretical calculation perspective[71]. They confirmed the feasibility of the $Ni^0/Ni^{II}/Ni^{I}/Ni^{III}/Ni^{I}$ cycle and identified the second OA is the rate-determining step.

Later, Liu *et al.* reported a similar reaction of aryl halides with vinyl bromides [Figure 6A] and further explored the mechanism of this reaction by a combination of experimental and DFT calculations, offering a more in-depth understanding[72]. Firstly, they conducted a control experiment using TEMPO (2,2,6,6-Tetramethylpiperidin-1-oxyl) to demonstrate that the reaction does not involve a radical chain process and that the participation of vinyl radicals is less likely. Next, a possible mechanism was determined through calculations, as shown in Figure 6B. The results revealed that the Ni^0 catalyst initially undergoes an OA process with vinyl bromides through the concerted two-electron, three-member transition state **TS2**, resulting in the formation of the vinyl Ni^{II} intermediate **IM7**. This intermediate is subsequently reduced by

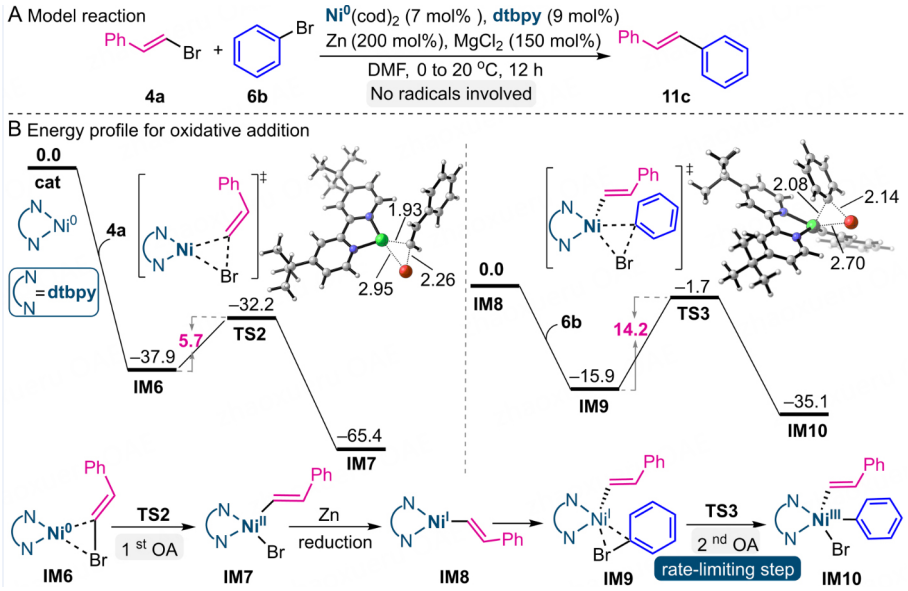

Figure 6. Computational mechanistic studies. (A) Model reaction used for DFT calculations; (B) Energy profile for oxidative addition process. Gibbs free energies are given in kcal/mol. Computations at the B3LYP-D3(BJ)/SDD for Ni, 6-311G(d,p) for Br, 6-31G(d,p) level. Selected bond distances are given in Å.

Zn to form the vinyl Ni^{I} intermediate **IM8**. The second OA involving bromobenzene then occurs via the transition state **TS3**, generating the Ni^{III} intermediate **IM10**. This process has an activation energy of 14.2 kcal/mol and constitutes the rate-determining step of the reaction.

Thereafter, Long *et al.* reported a similar mechanism for a reductive coupling of 2-Haloanilines[73]. They also discovered that the energy required for single-electron halide abstraction is less favorable than that of the two-electron OA process by 15.4 kcal/mol. This further implies that the formation of aryl radicals in this system is quite challenging. Recently, Long *et al.* developed a (bpy)Ni/Mn-catalyzed reductive coupling of 2-halophenol derivatives[74]. They successfully synthesized the Ni^{II} aryl intermediate through the reaction of Ni^{0} and aryl halides. Moreover, this intermediate was found to efficiently catalyze the reaction, leading to the desired coupling products. This observation suggests that the OA of Ni^{0} to aryl halides takes place in the catalytic cycle, and the resulting Ni^{II} aryl intermediate might be a key active species. All of the aforementioned findings indicate that the $Ni^{0}/Ni^{II}/Ni^{I}/Ni^{III}$ process is possible for Ni/(pyridine-type ligands)-catalyzed reductive couplings involving $C(sp^2)$ and $C(sp^2)$ electrophiles using Zn or Mn reductants.

According to Mechanism II, when involving $C(sp^3)$ electrophiles, a stepwise single-electron OA process can occur. Ren *et al.* revealed that the stepwise single-electron OA process between the Ni^{I} aryl intermediate **IM11** and CyBr **7b** is completed through the successive halogen atom abstraction transition state **TS4** and the radical addition transition state **TS5**[54] [Figure 7]. This process forms the Ni^{III} intermediate **IM12**, requiring relatively low activation energy barriers of 5.0 and 10.4 kcal/mol, respectively. A similar result was obtained for nickel-catalyzed reductive XC of activated primary amines with aryl halides, as reported by Yue *et al.*[75].

THE INVESTIGATION OF MECHANISM III

In general, a fundamental question in these catalytic systems is identifying the nature of the active catalyst at the outset of the reaction. Mechanism III is distinct from the previously discussed two mechanisms, as it is

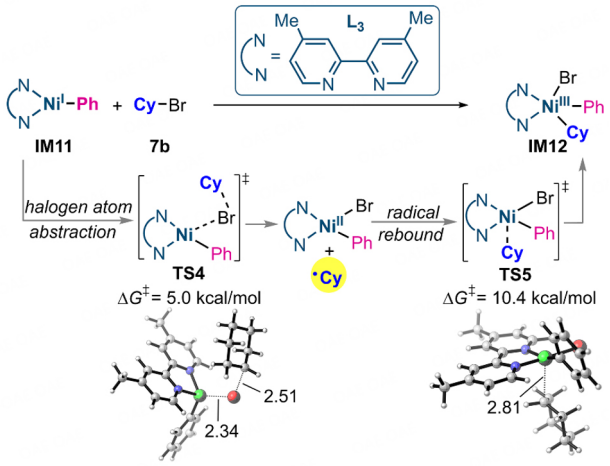

Figure 7. Stepwise single-electron oxidative addition process. Computations at the B3LYP/6-31g* level. Selected bond distances are given in Å.

characterized by the absence of Ni^0 throughout the entire process, with Ni^I species serving as the active catalyst. As illustrated in Scheme 4, starting from the active catalyst LNi^IX, the reaction can proceed through two distinct OA pathways. The first possibility involves a bimolecular OA to form $LNi^{II}X(R^1)$, while the second involves a single-molecule process that yields $LNi^{III}(X)_2(R^1)$. These two intermediates are then reduced to $LNi^I(R^1)$, followed by halogen atom abstraction to form R^2 radical and $LNi^{II}X(R^1)$, which, upon radical rebound, produce $LNi^{III}(X)(R^1)(R^2)$. Finally, RE occurs, leading to the formation of the product and regeneration of the active catalyst. Generally speaking, in the reductive coupling system involving $C(sp^2)$ and $C(sp^3)$ electrophiles, catalyzed by Ni catalyst and pyridine-type nitrogen ligands, it has been observed that when the substrates change to alkyl halides featuring more complex structures, such as alkenes and heteroatoms, the reaction mechanism tends to shift towards Mechanism III.

This mechanism was corroborated through various experimental mechanistic investigations, including kinetic, spectroscopic, and organometallic studies, conducted by Lin *et al.*[76]. They used the model reaction depicted in Figure 8A, where aryl bromide **5a** and alkyl bromide **8b** can be effectively cross-coupled to generate product **12c** in the presence of Zn and $NiBr_2$·DME/1,10-phenanthroline. Firstly, they carried out substrate probe experiments to demonstrate the presence of radical intermediates in the system. Subsequently, the kinetic studies were performed, and the reaction order was obtained, as illustrated in Figure 8B. The zero-order dependence on substrates **5a** and **8b**, together with the first-order dependence on [Ni], and the observation that the reaction rate increases along with increasing agitation rate and Zn loading. Integrating these results suggests that the reduction of Ni by Zn is the rate-determining step of the reaction. After that, they identified Ni^{II} intermediates **IM13** and **IM14** as the catalyst resting state through EPR, ^1H NMR, and UV-visible spectroscopy analysis [Figure 8C]. In contrast to the previous system where Ni^0 served as the reducing species, the resting state **IM13** can only be reduced by Zn to Ni^I species **IM15**, which was confirmed by comparing its cyclic voltammetry (CV) and EPR data with those of isolated and X-ray characterized (phen*)Ni^IBr **IM16** (phen* = 2, 9-di-sec-butyl-phenanthroline) [Figure 8D]. Therefore, Ni^I Br **IM15** serves as the starting point for the reaction. Several reports have also demonstrated that the Ni^IX complex serves as the initial active catalyst in nickel-catalyzed reductive coupling reactions[77-80].

Subsequently, competition experiments were conducted to explore the electrophile activation of substrates [Figure 8E]. The reaction rates of **5a** and **8b** with **IM15** were 1.2 and 0.42 mM/min, respectively, indicating

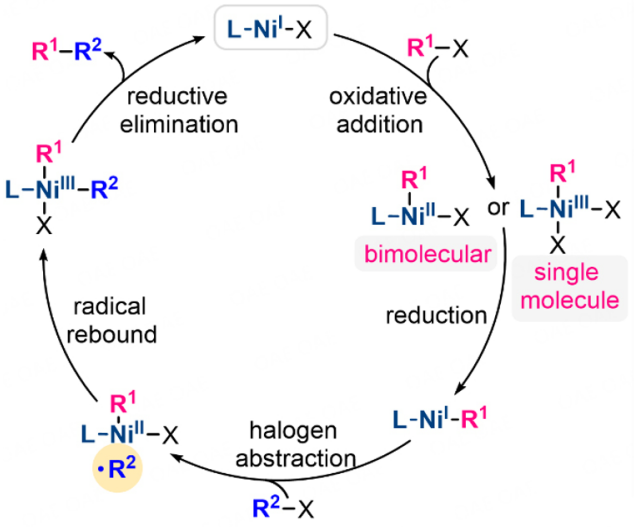

Scheme 4. The catalytic cycle of Mechanism III.

that the OA of Ni^{I}Br with PhBr is faster than its reaction with haloalkanes to generate radicals. They speculate that the OA process takes precedence over radical formation. These findings contradict the results proposed by the radical chain mechanism, which suggests that Ni^{I}Br preferentially activates alkyl halides to generate radicals, occurring prior to OA. It is important to note that Ting *et al.* further demonstrated that aryl halides undergo OA with Ni^{I} halide complexes through quantitative experiments, in which they obtained structurally characterized bipyridine-ligated Ni^{III} aryl complexes[81]. In addition, Till *et al.* discovered that (dtbpy)Ni^{I}Br can be generated through pulse radiolysis, and it is capable of undergoing OA with aryl halides[82]. Then, Breitenfeld *et al.* performed stoichiometric experiments to demonstrate that **6a** *o*-TolBr reacts with **IM15** via bimolecular OA, leading to **IM13** and **IM17**[83,84] [Figure 8F]. EPR spectroscopy reveals that **IM17** can also only be reduced by Zn to form Ni^{I} aryl species. Similar structures of (IPr)Ni^{I} alkyl and aryl complexes have been characterized by Laskowski *et al.*, and they confirmed that Ni^{I} alkyl species can activate alkyl halides via a radical process[85]. In order to identify how Ni^{II} aryl intermediate interacts with substrate **8b**, an array of control experiments was carried out [Figure 8G] . Stoichiometric experiments have shown that the efficiency of the reaction is low in the absence of Zn, with only 30% of **8b** being converted (entry 1). However, with the addition of Zn, the conversion of **8b** increases to 100% (entry 2), suggesting that Zn plays a crucial role in promoting the reaction. This finding contrasts with the results reported by Weix, where the reaction could efficiently yield the desired product even without Zn. Moreover, the formation of **14c** infers the existence of the radical intermediate that undergoes cyclization and dimerization, while the cross-coupled product **15c** is obtained through a radical addition and reduction elimination process. They also found that when the substituent Ar is *o*-Tol, both **15c** and **14c** can be obtained (entry 2). When the substituent is Mes, only dimer **14c** can be formed (entry 3). This suggests that the larger steric hindrance prevents radical addition to Ni center. Taken together, these results are consistent with Mechanism III.

By comparing the catalytic systems of Weix and Diao, significant differences were found. (1) The types of electrophilic substrates used are different: Weix employed simple linear alkyl halides such as iodobenzene,

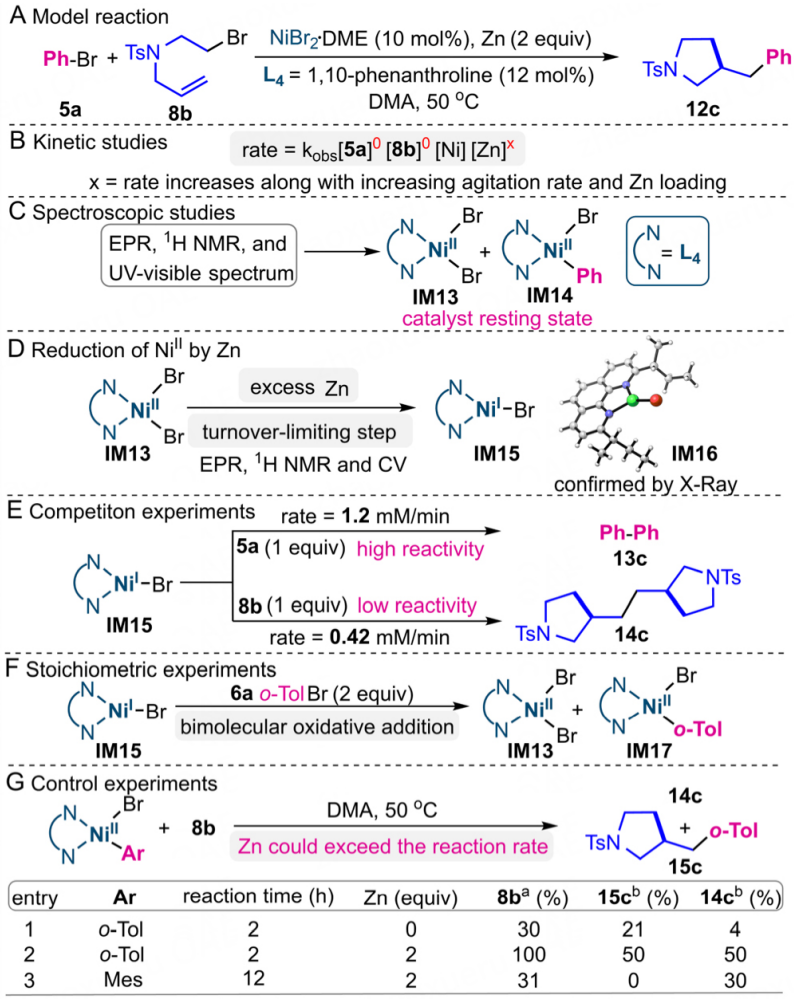

entry	Ar	reaction time (h)	Zn (equiv)	8b[a] (%)	15c[b] (%)	14c[b] (%)
1	*o*-Tol	2	0	30	21	4
2	*o*-Tol	2	2	100	50	50
3	Mes	12	2	31	0	30

Figure 8. Experimental mechanistic investigations of Mechanism III. (A) Model reaction used for mechanistic investigations; (B) Kinetic studies of model reaction; (C) Spectroscopic studies; (D) Reduction of Ni^{II} by Zn; (E) Competition experiments between **5a** and **8b**; (F) Stoichiometric experiments; (G) Control experiments. [a] and [b]: refer to conversion and yields, respectively; DMA: N, N-dimethylacetamide, DME: 1,2-Dimethoxyethane.

while Diao used structurally complex alkyl halides substituted with heteroatoms and olefins; (2) The ligands used are different: although both ligands belong to the pyridine-type nitrogen ligands, they have different substitution patterns, one being a bipyridine and the other being a phenanthroline; (3) The reducing agents used are different: Weix used Mn, while Diao used Zn. These differences in catalytic systems are important factors that lead to changes in the reaction mechanism. More importantly, Ju *et al.* discovered that the use of biOx ligand excludes the reduction step of $(biOx)Ni^{II}$[86]. This can be attributed to the lack of ligand redox activity, resulting in more negative reduction potentials of $(biOx)Ni^{II}$ complexes, rendering them unable to be reduced by Zn and Mn. This further highlights the significant impact of ligands on the mechanism[87].

Similar to Weix, Diao found that the cross-selectivity also originates from the different activation sequences of the two electrophiles. Unlike the Weix's system, which utilizes Ni^0 and Ni^{II} species, Diao employs $Ni^{I}Br$ and $Ni^{I}Ph$ to activate different electrophiles, respectively. Specifically, the OA is mainly influenced by steric effects, while the formation of radicals via halogen-atom abstraction is related to electronic effects. Therefore, sterically assessable $Ni^{I}Br$ preferentially undergoes two-electron OA with PhBr **5a** to give $C(sp^2)$ Ni^{II} species, while electron-rich but sterically hindered $Ni^{I}Ph$ predominantly activates alkyl bromides **8b** via

halogen-atom abstraction to forms C(sp^3) radicals [Figure 9], thus resulting in cross-selectivity.

Meanwhile, by combining experimental and DFT calculations, Shu *et al.* investigated the mechanism of dipyridine-ligated nickel-catalyzed reductive dicarbofunctionalization of propene with tert-butyl iodide and iodobenzene with the use of Zn reductants[88]. Their findings confirmed the feasibility of the pathway involving Ni^{I} species. More recently, Zhu *et al.* developed an RCC reaction of α-oxy halides enabled by Mn reductants, photocatalysis, electrocatalysis, or mechanochemistry in the presence of nickel and phenanthroline ligands[89]. Surprisingly, through detailed experimental and theoretical studies, they found the mechanisms of all four catalytic systems are consistent with Mechanism III. Besides, they noted that the Ni^{III} intermediate, obtained through OA, may trigger comproportionation with Ni^{I} species to afford the Ni^{II} intermediate. Intriguingly, Day *et al.* disclosed that polypyridine-ligated Ni^{II} halide complexes can undergo the comproportionation with Ni^{0} to form Ni^{I} species[90]. These electron-transfer events were corroborated by electrochemical techniques and detailed quantum mechanical calculations. It is worth noting that Tang *et al.* conducted comprehensive mechanistic studies on the OA of Ni(I) to aryl iodides using electroanalytical and statistical modeling techniques[91]. And predicted OA rates can be utilized not only to interpret observed reactivities but also to rationalize the mechanism. This indicates that an expanding array of techniques can assist us in predicting reaction models, understanding reaction mechanisms, and guiding the design of novel catalytic systems.

THE INVESTIGATION OF MECHANISM IV

In contrast to the aforementioned initial three mechanisms, Mechanism IV fundamentally encompasses an S_N2 process and the Ni^{0}/Ni^{II} catalytic cycle. As depicted in Scheme 5, commencing with Ni^{0}, the reaction proceeds sequentially through OA, TM, an S_N2 reaction, a second TM, and ultimately RE. Notably, this particular mechanism employs organic Grignard reagents as reductants, as opposed to their conventional use as coupling reagents, thereby deviating significantly from traditional XC reactions. Mechanism IV is chiefly observed in the intramolecular reductive coupling reaction system, which is facilitated by Ni^{0} catalysts in the presence of phosphine ligands and organic Grignard reagents. The primary substrates for this mechanism encompass a range of active pyrrole and amine derivatives. It is important to note that Mechanism IV demonstrates fundamental differences in terms of reaction conditions and substrates when contrasted with the previously discussed three mechanisms.

Chen *et al.* conducted a comprehensive mechanistic investigation on Ni^{0}/BINAP-catalyzed stereospecific intramolecular RCC reactions of benzylic ethers through a combination of experimental and computational approaches, thereby confirming the feasibility of this particular mechanism[92]. In this discussion, we concentrate on the key transition states for the product formation, as illustrated in Figure 10A. The reaction proceeds sequentially through the OA transition state **TS6**, TM transition state **TS7** and intramolecular S_N2-like attack transition state **TS8** to achieve C–O bond cleavage, alkyl transfer, and C–Cl bond cleavage, ultimately leading to the product **16c**. The energy barriers associated with these steps are 21.9, 12.0, and 9.3 kcal/mol, respectively. This process takes place under a closed-shell system without involving radicals and exhibits stereospecificity. Among these steps, the OA of the C–O bond occurs with stereoinversion of the benzylic stereogenic center, which is facilitated by the assistance of Grignard reagents, constituting the rate- and selectivity-determining step for product formation. Concurrently, they performed a ^{13}C KIE study of the benzylic ether of 2-naphthyltetrahydropyran **9b**, which revealed a significant (> 1.01) KIE numerical distribution for benzylic C11 compared to other atoms [Figure 10B]. This further substantiated that the activation of the C–O bond is the rate-determining step.

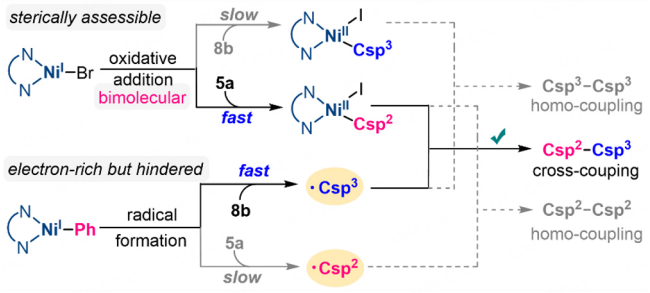

Figure 9. The origin of the cross-selectivity.

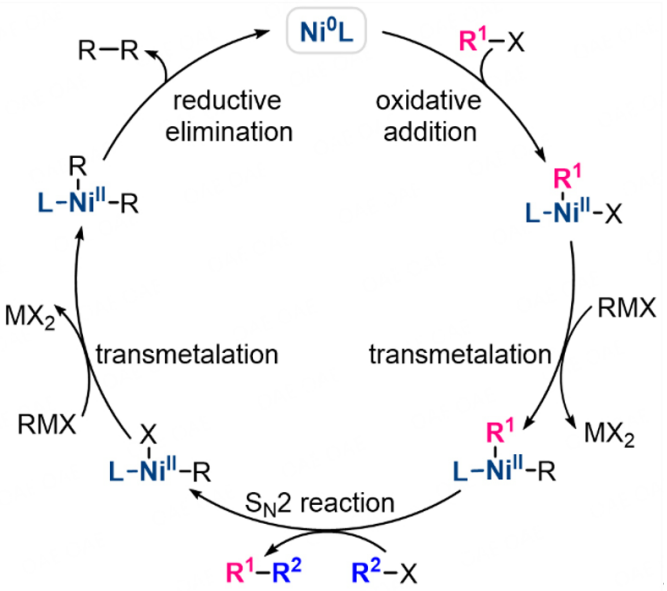

Scheme 5. The catalytic cycle of Mechanism IV.

Moreover, the activation of both the C–O and C–Cl bonds collectively control the stereospecificity of overall reactions.

They also discovered that the intramolecular reductive coupling reaction of halogenated sulfonylamine derivatives, catalyzed by air-stable ((*R*)-BINAP)$NiCl_2$ and MeMgI organic Grignard reagents, still adheres to the Ni^0/Ni^{II} catalytic cycle[93,94]. Furthermore, Xu *et al.* conducted a detailed theoretical study on the Ni^0/XantPhos-catalyzed intramolecular reductive coupling of tetrahydropyrans, indicating that Mechanism IV is applicable to this system[95]. Similarly, nickel-catalyzed intramolecular reductive coupling of difluoromethyl moiety and benzylic ether, reported by Lucas *et al.*, also follows a comparable reaction mechanism[96]. It is noteworthy that Sanford *et al.* found that when utilizing non-cyclic 1,3-diol derivatives featuring two $C(sp^3)$–I bonds for intramolecular reductive coupling, the activation of $C(sp^3)$–I bonds proceeds via a radical pathway rather than the S_N2 mechanism[97]. This finding highlights the notion that the intrinsic characteristics of the substrates can indeed exert a substantial impact on the reaction mechanism.

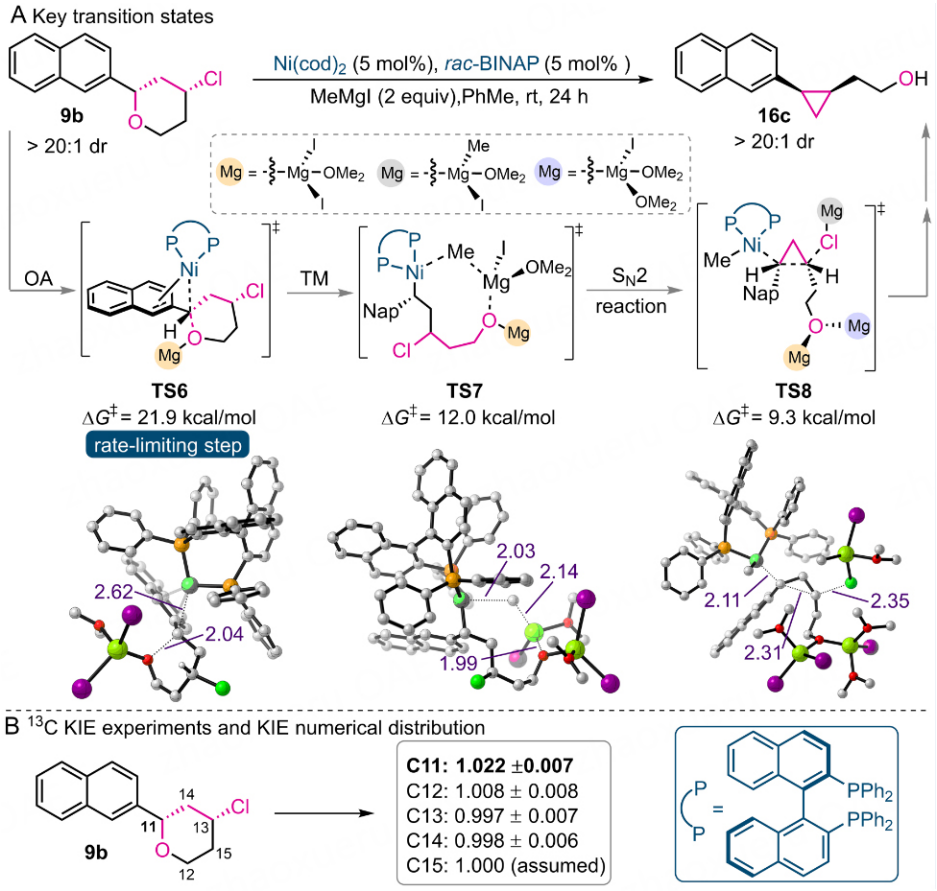

Figure 10. Experimental and computational mechanistic studies. (A) DFT calculations for key transition states; (B) ^{13}C KIE experiments and KIE numerical distribution of **9b**. Computations at the B3LYP-D3(BJ)-SMD/def2-TZVPP//B3LYP-D3(BJ)/def2-SVP level. Selected bond distances are given in Å. The hydrogen atom was omitted for simplification.

CONCLUSION AND OUTLOOK

In summary, nickel-catalyzed reductive coupling reactions exhibit considerable diversity in their mechanisms, distinct from those catalyzed by palladium and platinum. This can be ascribed to the unique characteristics of nickel, including high paring energy, low electronegativity and redox potential, and multiple oxidation states (0, I, II, III, IV)[35]. These enable nickel catalysts to preferentially undergo both two- and one-electron redox processes, leading to comparatively diverse mechanistic scenarios. Additionally, these mechanisms are closely related to substrates, ligands, and reducing conditions, making it challenging to discern a unifying pattern. From the four potential reaction mechanisms summarized, we can identify some basic trends: (1) C(sp^2) electrophiles tend to undergo two-electron OA, while C(sp^3) electrophiles prefer a single-electron pathway initiated by halogen atom transfer; (2) When nitrogen ligands are employed and C(sp^3) electrophiles are involved, the reaction is inclined to proceed via a radical pathway, whereas a closed-shell reaction generally occurs with phosphine ligands; (3) Reaction systems involving photoredox catalysts or electrocatalysis typically undergo a single-electron transfer process. However, determining the conceivable reaction mechanism requires considering various reaction conditions, such as the choice of ligands and substrates, and whether the reducing system involves conventional metal and organic reducing agents or emerging photoredox and electrocatalysis. It is particularly important to ascertain whether a Ni^{II} catalyst precursor is ultimately reduced to Ni^0 or Ni^I, as this determines the active catalyst in the reaction.

As for C(sp^2)–C(sp^3) XECs, the origin of the cross-selectivity over homo-selectivity can be ascribed to the different activation sequences of two electrophiles. Notably, different systems use different Ni species to activate electrophiles. For instance, in the Ni/dtbpy-catalyzed system for the XEC of iodobenzene with iodooctadecane, with Mn as the reducing agent, Ni^0 and Ni^II are always used to activate the electrophiles. In contrast, Ni^IBr and Ni^IPh species can activate electrophiles when using more complex alkyl bromide containing olefins and heteroatoms substrate, Zn reductants, and 1,10-phenanthroline ligands. Generally speaking, due to the favorable π-metal interactions and the instability of aryl radicals, C(sp^2) electrophiles tend to proceed through OA, while C(sp^3) electrophiles are more likely to generate radicals. Additionally, OA and radical formation processes are also influenced by steric hindrance and electronic effects, respectively.

Despite significant progress made by both experimental and theoretical studies in characterizing the structures of key intermediates, providing reaction rates, identifying the activation modes of electrophiles, determining rate- or selectivity-determining steps, and identifying the origin of cross-selectivity, several limitations and challenges in mechanistic studies remain to be addressed: (1) There are limited studies on the mechanism of RCC reactions, especially those involving photoredox and electrochemistry catalysis; (2) The electron transfer process involved in the reduction process is still unclear; (3) So far, there is no data-driven and artificial intelligence linkages to aid further mechanistic exploration and reaction prediction. Therefore, the mechanistic investigation of nickel-catalyzed reductive couplings is far from complete, and concerted endeavors of experimental and computational studies are highly demanded to help chemists design more powerful and novel catalytic systems.

DECLARATIONS

Acknowledgments

We sincerely thank all the leading chemists and co-workers who have contributed to the methodological developments and mechanistic studies of nickel-catalyzed reduction cross-couplings.

Authors' contributions

Guided this work, gave valuable suggestions and discussion for the review, and revised the paper: Zhang SQ, Hong X

Wrote the paper: Wu H

Availability of data and materials

Not applicable.

Financial support and sponsorship

This work was supported by the National Natural Science Foundation of China (22122109 and 22271253, Hong X; 22103070, Zhang SQ); National Key R&D Program of China (2022YFA1504301, Hong X); Zhejiang Provincial Natural Science Foundation of China under Grant No. LDQ23B020002 (Hong X); the Starry Night Science Fund of Zhejiang University Shanghai Institute for Advanced Study (SN-ZJU-SIAS-006, Hong X); Beijing National Laboratory for Molecular Sciences (BNLMS202102, Hong X); CAS Youth Interdisciplinary Team (JCTD-2021-11, Hong X); Fundamental Research Funds for the Central Universities (226-2022-00140, 226-2022-00224 and 226-2023-00115, Hong X); the Center of Chemistry for Frontier Technologies and Key Laboratory of Precise Synthesis of Functional Molecules of Zhejiang Province (PSFM 2021-01, Hong X); the State Key Laboratory of Clean Energy Utilization (ZJUCEU2020007, Hong X); the State Key Laboratory of Physical Chemistry of Solid Surfaces (202210, Hong X); the Leading Innovation Team grant from Department of Science and Technology of Zhejiang Province (2022R01005, Hong X) are gratefully acknowledged. Calculations were performed on the high-performance computing system at the

Department of Chemistry, Zhejiang University.

Conflicts of interest

All authors declared that there are no conflicts of interest.

Ethical approval and consent to participate

Not applicable.

Consent for publication

Not applicable.

Copyright

REFERENCES

1. Lucas EL, Jarvo ER. Stereospecific and stereoconvergent cross-couplings between alkyl electrophiles. *Nat Rev Chem* 2017;1:0065. DOI
2. Poremba KE, Dibrell SE, Reisman SE. Nickel-catalyzed enantioselective reductive cross-coupling reactions. *ACS Catal* 2020;10:8237-46. DOI PubMed PMC
3. Wang X, Dai Y, Gong H. Nickel-catalyzed reductive couplings. *Top Curr Chem* 2016;374:43. DOI PubMed
4. Liu J, Ye Y, Sessler JL, Gong H. Cross-electrophile couplings of activated and sterically hindered halides and alcohol derivatives. *Acc Chem Res* 2020;53:1833-45. DOI
5. Ni S, Li CX, Mao Y, et al. Ni-catalyzed deaminative cross-electrophile coupling of Katritzky salts with halides via C─N bond activation. *Sci Adv* 2019;5:eaaw9516. DOI PubMed PMC
6. Xue W, Jia X, Wang X, Tao X, Yin Z, Gong H. Nickel-catalyzed formation of quaternary carbon centers using tertiary alkyl electrophiles. *Chem Soc Rev* 2021;50:4162-84. DOI
7. Pang X, Su PF, Shu XZ. Reductive cross-coupling of unreactive electrophiles. *Acc Chem Res* 2022;55:2491-509. DOI PubMed
8. Yi L, Ji T, Chen K, Chen X, Rueping M. Nickel-catalyzed reductive cross-couplings: new opportunities for carbon-carbon bond formations through photochemistry and electrochemistry. *CCS Chem* 2022;4:9-30. DOI
9. Durandetti M, Gosmini C, Périchon J. Ni-catalyzed activation of α-chloroesters: a simple method for the synthesis of α-arylesters and β -hydroxyesters. *Tetrahedron* 2007;63:1146-53. DOI
10. Ye Y, Qi X, Xu B, et al. Nickel-catalyzed cross-electrophile allylation of vinyl bromides and the modification of anti-tumour natural medicine β-elemene. *Chem Sci* 2022;13:6959-66. DOI PubMed PMC
11. Charboneau DJ, Hazari N, Huang H, Uehling MR, Zultanski SL. Homogeneous organic electron donors in nickel-catalyzed reductive transformations. *J Org Chem* 2022;87:7589-609. DOI PubMed PMC
12. Charboneau DJ, Huang H, Barth EL, et al. Tunable and practical homogeneous organic reductants for cross-electrophile coupling. *J Am Chem Soc* 2021;143:21024-36. DOI PubMed PMC
13. Zhou J, Wang D, Xu W, Hu Z, Xu T. Enantioselective C(sp^3)-C(sp^3) reductive cross-electrophile coupling of unactivated alkyl halides with α-Chloroboronates via dual nickel/photoredox catalysis. *J Am Chem Soc* 2023;145:2081-7. DOI
14. Zhang P, Le CC, MacMillan DW. Silyl radical activation of alkyl halides in metallaphotoredox catalysis: a unique pathway for cross-electrophile coupling. *J Am Chem Soc* 2016;138:8084-7. DOI PubMed PMC
15. Dongbang S, Doyle AG. Ni/photoredox-catalyzed C(sp^3)-C(sp^3) coupling between aziridines and acetals as alcohol-derived alkyl radical precursors. *J Am Chem Soc* 2022;144:20067-77. DOI PubMed PMC
16. Bacauanu V, Cardinal S, Yamauchi M, et al. Metallaphotoredox difluoromethylation of aryl bromides. *Angew Chem Int Ed Engl* 2018;57:12543-8. DOI PubMed
17. Yang T, Wei Y, Koh MJ. Photoinduced nickel-catalyzed deaminative cross-electrophile coupling for C(sp^2)–C(sp^3) and C(sp^3)–C(sp^3) bond formation. *ACS Catal* 2021;11:6519-25. DOI
18. Liu Y, Tao X, Mao Y, et al. Electrochemical C-N bond activation for deaminative reductive coupling of Katritzky salts. *Nat Commun* 2021;12:6745. DOI PubMed PMC
19. Liu D, Liu ZR, Wang ZH, et al. Paired electrolysis-enabled nickel-catalyzed enantioselective reductive cross-coupling between α-chloroesters and aryl bromides. *Nat Commun* 2022;13:7318. DOI PubMed PMC
20. Zackasee JLS, Zubaydi SA, Truesdell BL, Sevov CS. Synergistic catalyst-mediator pairings for electroreductive cross-electrophile coupling reactions. *ACS Catal* 2022;12:1161-6. DOI PubMed PMC
21. Perkins RJ, Pedro DJ, Hansen EC. Electrochemical Nickel Catalysis for Sp^2-Sp^3 cross-electrophile coupling reactions of unactivated alkyl halides. *Org Lett* 2017;19:3755-8. DOI
22. Hu X, Cheng-Sánchez I, Cuesta-Galisteo S, Nevado C. Nickel-catalyzed enantioselective electrochemical reductive cross-coupling of aryl aziridines with alkenyl bromides. *J Am Chem Soc* 2023;145:6270-9. DOI PubMed PMC

23. Zhang B, Gao Y, Hioki Y, et al. Ni-electrocatalytic Csp^3-Csp^3 doubly decarboxylative coupling. *Nature* 2022;606:313-8. DOI PubMed PMC
24. Nohira I, Chatani N. Nickel-catalyzed cross-electrophile coupling between C(sp^2)-F and C(sp^2)-Cl bonds by the reaction of *ortho*-fluoro-aromatic amides with aryl chlorides. *ACS Catal* 2021;11:4644-9. DOI
25. Ni S, Zhang W, Mei H, Han J, Pan Y. Ni-catalyzed reductive cross-coupling of amides with aryl iodide electrophiles via C-N bond activation. *Org Lett* 2017;19:2536-9. DOI
26. Zhu Z, Gong Y, Tong W, Xue W, Gong H. Ni-catalyzed cross-electrophile coupling of aryl triflates with thiocarbonates via C-O/C-O bond cleavage. *Org Lett* 2021;23:2158-63. DOI PubMed
27. Zhao C, Jia X, Wang X, Gong H. Ni-catalyzed reductive coupling of alkyl acids with unactivated tertiary alkyl and glycosyl halides. *J Am Chem Soc* 2014;136:17645-51. DOI
28. Kim S, Goldfogel MJ, Gilbert MM, Weix DJ. Nickel-catalyzed cross-electrophile coupling of aryl chlorides with primary alkyl chlorides. *J Am Chem Soc* 2020;142:9902-7. DOI PubMed PMC
29. Guo P, Wang K, Jin WJ, et al. Dynamic kinetic cross-electrophile arylation of benzyl alcohols by nickel catalysis. *J Am Chem Soc* 2021;143:513-23. DOI
30. Zhu Z, Lin L, Xiao J, Shi Z. Nickel-catalyzed stereo- and enantioselective cross-coupling of gem-difluoroalkenes with carbon electrophiles by C-F bond activation. *Angew Chem Int Ed Engl* 2022;61:e202113209. DOI PubMed
31. Chi BK, Widness JK, Gilbert MM, Salgueiro DC, Garcia KJ, Weix DJ. In-situ bromination enables formal cross-electrophile coupling of alcohols with aryl and alkenyl halides. *ACS Catal* 2022;12:580-6. DOI PubMed PMC
32. Lin T, Gu Y, Qian P, Guan H, Walsh PJ, Mao J. Nickel-catalyzed reductive coupling of homoenolates and their higher homologues with unactivated alkyl bromides. *Nat Commun* 2020;11:5638. DOI PubMed PMC
33. Kang K, Weix DJ. Nickel-catalyzed C(sp^3)-C(sp^3) cross-electrophile coupling of in situ generated nhp esters with unactivated alkyl bromides. *Org Lett* 2022;24:2853-7. DOI PubMed PMC
34. Cui N, Lin T, Wang YE, et al. Nickel-catalyzed reductive coupling of γ-metalated ketones with unactivated alkyl bromides. *Org Lett* 2022;24:3987-92. DOI
35. Diccianni JB, Diao T. Mechanisms of nickel-catalyzed cross-coupling reactions. *Trends Chem* 2019;1:830-44. DOI
36. Hu X. Nickel-catalyzed cross coupling of non-activated alkyl halides: a mechanistic perspective. *Chem Sci* 2011;2:1867-86. DOI
37. Everson DA, Weix DJ. Cross-electrophile coupling: principles of reactivity and selectivity. *J Org Chem* 2014;79:4793-8. DOI PubMed PMC
38. Weix DJ. Methods and mechanisms for cross-electrophile coupling of Csp^2 halides with alkyl electrophiles. *Acc Chem Res* 2015;48:1767-75. DOI PubMed PMC
39. Diccianni J, Lin Q, Diao T. Mechanisms of nickel-catalyzed coupling reactions and applications in alkene functionalization. *Acc Chem Res* 2020;53:906-19. DOI PubMed PMC
40. Yang T, Jiang Y, Luo Y, Lim JJH, Lan Y, Koh MJ. Chemoselective union of olefins, organohalides, and redox-active esters enables regioselective alkene dialkylation. *J Am Chem Soc* 2020;142:21410-9. DOI PubMed
41. Duan A, Xiao F, Lan Y, Niu L. Mechanistic views and computational studies on transition-metal-catalyzed reductive coupling reactions. *Chem Soc Rev* 2022;51:9986-10015. DOI PubMed
42. Wang Y, Ren Q. DFT study of the mechanisms of transition-metal-catalyzed reductive coupling reactions. *Curr Org Chem* 2020;24:1367-83. DOI
43. Gu J, Wang X, Xue W, Gong H. Nickel-catalyzed reductive coupling of alkyl halides with other electrophiles: concept and mechanistic considerations. *Org Chem Front* 2015;2:1411-21. DOI
44. Zhang SQ, Hong X. Mechanism and selectivity control in Ni- and Pd-catalyzed cross-couplings involving carbon-oxygen bond activation. *Acc Chem Res* 2021;54:2158-71. DOI PubMed
45. Gutierrez O, Tellis JC, Primer DN, Molander GA, Kozlowski MC. Nickel-catalyzed cross-coupling of photoredox-generated radicals: uncovering a general manifold for stereoconvergence in nickel-catalyzed cross-couplings. *J Am Chem Soc* 2015;137:4896-9. DOI PubMed PMC
46. Kolahdouzan K, Khalaf R, Grandner JM, Chen Y, Terrett JA, Huestis MP. Dual photoredox/nickel-catalyzed conversion of aryl halides to aryl aminooxetanes: computational evidence for a substrate-dependent switch in mechanism. *ACS Catal* 2020;10:405-11. DOI
47. Xu J, Yang Y, Zhao X, Liu C, Zhang D. DFT mechanistic study of Ir^{III}/Ni^{II}-metallaphotoredox-catalyzed difluoromethylation of aryl bromides. *Inorg Chem* 2021;60:8682-91. DOI
48. Biswas S, Weix DJ. Mechanism and selectivity in nickel-catalyzed cross-electrophile coupling of aryl halides with alkyl halides. *J Am Chem Soc* 2013;135:16192-7. DOI PubMed PMC
49. Everson DA, Shrestha R, Weix DJ. Nickel-catalyzed reductive cross-coupling of aryl halides with alkyl halides. *J Am Chem Soc* 2010;132:920-1. DOI PubMed
50. Everson DA, Jones BA, Weix DJ. Replacing conventional carbon nucleophiles with electrophiles: nickel-catalyzed reductive alkylation of aryl bromides and chlorides. *J Am Chem Soc* 2012;134:6146-59. DOI PubMed PMC
51. Wotal AC, Ribson RD, Weix DJ. Stoichiometric reactions of acylnickel^{II} complexes with electrophiles and the catalytic synthesis of ketones. *Organometallics* 2014;33:5874-81. DOI PubMed PMC
52. Sheng J, Ni HQ, Zhang HR, Zhang KF, Wang YN, Wang XS. Nickel-catalyzed reductive cross-coupling of aryl halides with

monofluoroalkyl halides for late-stage monofluoroalkylation. *Angew Chem Int Ed Engl* 2018;57:7634-9. DOI PubMed
53. Brauer DJ, Krueger C. Bonding of aromatic hydrocarbons to nickel (0). Structure of bis (tricyclohexylphosphine)(1,2-.eta.2-anthracene) nickel (0)-toluene. *Inorg Chem* 1977;16:884-91. DOI
54. Ren Q, Jiang F, Gong H. DFT study of the single electron transfer mechanisms in Ni-Catalyzed reductive cross-coupling of aryl bromide and alkyl bromide. *J Organomet Chem* 2014;770:130-5. DOI
55. Kumar GS, Peshkov A, Brzozowska A, Nikolaienko P, Zhu C, Rueping M. Nickel-catalyzed chain-walking cross-electrophile coupling of alkyl and aryl halides and olefin hydroarylation enabled by electrochemical reduction. *Angew Chem Int Ed Engl* 2020;59:6513-9. DOI PubMed
56. Wang X, Ma G, Peng Y, et al. Ni-catalyzed reductive coupling of electron-rich aryl iodides with tertiary alkyl halides. *J Am Chem Soc* 2018;140:14490-7. DOI
57. Ji H, Lin D, Tai L, et al. Nickel-catalyzed enantioselective coupling of acid chlorides with α-bromobenzoates: an asymmetric acyloin synthesis. *J Am Chem Soc* 2022;144:23019-29. DOI
58. Guan H, Zhang Q, Walsh PJ, Mao J. Nickel/photoredox-catalyzed asymmetric reductive cross-coupling of racemic α-chloro esters with aryl iodides. *Angew Chem Int Ed Engl* 2020;59:5172-7. DOI PubMed
59. Lau SH, Borden MA, Steiman TJ, Wang LS, Parasram M, Doyle AG. Ni/photoredox-catalyzed enantioselective cross-electrophile coupling of styrene oxides with aryl iodides. *J Am Chem Soc* 2021;143:15873-81. DOI PubMed PMC
60. Wang H, Zheng P, Wu X, Li Y, Xu T. Modular and facile access to chiral α-aryl phosphates via dual nickel- and photoredox-catalyzed reductive cross-coupling. *J Am Chem Soc* 2022;144:3989-97. DOI
61. Yuan M, Song Z, Badir SO, Molander GA, Gutierrez O. On the nature of $C(sp^3)$- $C(sp^2)$ bond formation in nickel-catalyzed tertiary radical cross-couplings: a case study of Ni/photoredox catalytic cross-coupling of alkyl radicals and aryl halides. *J Am Chem Soc* 2020;142:7225-34. DOI PubMed PMC
62. Paul A, Smith MD, Vannucci AK. Photoredox-assisted reductive cross-coupling: mechanistic insight into catalytic aryl-alkyl cross-couplings. *J Org Chem* 2017;82:1996-2003. DOI
63. Hamby TB, LaLama MJ, Sevov CS. Controlling Ni redox states by dynamic ligand exchange for electroreductive Csp^3-Csp^2 coupling. *Science* 2022;376:410-6. DOI PubMed PMC
64. Li Z, Sun W, Wang X, Li L, Zhang Y, Li C. Electrochemically enabled, nickel-catalyzed dehydroxylative cross-coupling of alcohols with aryl halides. *J Am Chem Soc* 2021;143:3536-43. DOI
65. Diccianni JB, Katigbak J, Hu C, Diao T. Mechanistic characterization of (Xantphos)Ni(I)-mediated alkyl bromide activation: oxidative addition, electron transfer, or halogen-atom abstraction. *J Am Chem Soc* 2019;141:1788-96. DOI PubMed
66. Funes-Ardoiz I, Nelson DJ, Maseras F. halide abstraction competes with oxidative addition in the reactions of aryl halides with $[Ni(PMe_n Ph_{(3-n)})_4]$. *Chemistry* 2017;23:16728-33. DOI PubMed PMC
67. Kehoe R, Mahadevan M, Manzoor A, et al. Reactions of the Ni(0) Compound $Ni(PPh_3)_4$ with unactivated alkyl halides: oxidative addition reactions involving radical processes and nickel(I) intermediates. *Organometallics* 2018;37:2450-67. DOI
68. Yoo C, Ajitha MJ, Jung Y, Lee Y. Mechanistic study on C-C bond formation of a nickel(I) monocarbonyl species with alkyl iodides: experimental and computational investigations. *Organometallics* 2015;34:4305-11. DOI
69. Lin Q, Fu Y, Liu P, Diao T. Monovalent nickel-mediated radical formation: a concerted halogen-atom dissociation pathway determined by electroanalytical studies. *J Am Chem Soc* 2021;143:14196-206. DOI PubMed PMC
70. Guo L, Yuan M, Zhang Y, et al. General method for enantioselective three-component carboarylation of alkenes enabled by visible-light dual photoredox/nickel catalysis. *J Am Chem Soc* 2020;142:20390-9. DOI
71. Jiang F, Ren Q. Theoretical investigation of the mechanisms of the biphenyl formation in Ni-catalyzed reductive cross-coupling system. *J Organomet Chem* 2014;757:72-8. DOI
72. Liu J, Ren Q, Zhang X, Gong H. Preparation of vinyl arenes by nickel-catalyzed reductive coupling of aryl halides with vinyl bromides. *Angew Chem Int Ed Engl* 2016;55:15544-8. DOI
73. Long C, Ni S, Su M, Wang X, Tan W. Highly chemoselective access to 2,2′-diaminobiaryls via Ni-catalyzed protecting-group-free coupling of 2-haloanilines. *ACS Catal* 2020;10:13641-9. DOI
74. Long CY, Chen H, Ma C, et al. Highly chemoselective Ni-catalyzed protecting-group-free 2,2'-biphenol synthesis and mechanistic insights. *Org Lett* 2022;24:4155-9. DOI
75. Yue H, Zhu C, Shen L, et al. Nickel-catalyzed C-N bond activation: activated primary amines as alkylating reagents in reductive cross-coupling. *Chem Sci* 2019;10:4430-5. DOI PubMed PMC
76. Lin Q, Diao T. Mechanism of Ni-catalyzed reductive 1,2-dicarbofunctionalization of alkenes. *J Am Chem Soc* 2019;141:17937-48. DOI PubMed PMC
77. Cornella J, Gómez-Bengoa E, Martin R. Combined experimental and theoretical study on the reductive cleavage of inert C-O bonds with silanes: ruling out a classical Ni(0)/Ni(II) catalytic couple and evidence for Ni(I) intermediates. *J Am Chem Soc* 2013;135:1997-2009. DOI
78. Chen H, Yue H, Zhu C, Rueping M. Reactivity in nickel-catalyzed multi-component sequential reductive cross-coupling reactions. *Angew Chem Int Ed Engl* 2022;61:e202204144. DOI
79. Wang X, Ma Y, Ye J, Liu Z, Cheng R. Theoretical investigation of mechanism on nickel-catalyzed electrochemical cross-coupling of aryl bromides and arylamines. *Catal Sci Technol* 2023;13:1032-40. DOI
80. Tang T, Jones E, Wild T, Hazra A, Minteer SD, Sigman MS. Investigating oxidative addition mechanisms of allylic electrophiles with

low-valent Ni/Co catalysts using electroanalytical and data science techniques. *J Am Chem Soc* 2022;144:20056-66. DOI PubMed

81. Ting SI, Williams WL, Doyle AG. Oxidative addition of aryl halides to a Ni(I)-bipyridine complex. *J Am Chem Soc* 2022;144:5575-82. DOI PubMed
82. Till NA, Oh S, MacMillan DWC, Bird MJ. The application of pulse radiolysis to the study of Ni(I) intermediates in ni-catalyzed cross-coupling reactions. *J Am Chem Soc* 2021;143:9332-7. DOI
83. Breitenfeld J, Wodrich MD, Hu X. Bimetallic oxidative addition in nickel-catalyzed alkyl-aryl kumada coupling reactions. *Organometallics* 2014;33:5708-15. DOI
84. Breitenfeld J, Ruiz J, Wodrich MD, Hu X. Bimetallic oxidative addition involving radical intermediates in nickel-catalyzed alkyl-alkyl kumada coupling reactions. *J Am Chem Soc* 2013;135:12004-12. DOI PubMed
85. Laskowski CA, Bungum DJ, Baldwin SM, Del Ciello SA, Iluc VM, Hillhouse GL. Synthesis and reactivity of two-coordinate Ni(I) alkyl and aryl complexes. *J Am Chem Soc* 2013;135:18272-5. DOI PubMed
86. Ju L, Lin Q, LiBretto NJ, et al. Reactivity of (bi-Oxazoline)organonickel complexes and revision of a catalytic mechanism. *J Am Chem Soc* 2021;143:14458-63. DOI PubMed PMC
87. Thane TA, Jarvo ER. Ligand-based control of nickel catalysts: switching chemoselectivity from one-electron to two-electron pathways in competing reactions of 4-halotetrahydropyrans. *Org Lett* 2022;24:5003-8. DOI PubMed
88. Shu W, García-Domínguez A, Quirós MT, Mondal R, Cárdenas DJ, Nevado C. Ni-catalyzed reductive dicarbofunctionalization of nonactivated alkenes: scope and mechanistic insights. *J Am Chem Soc* 2019;141:13812-21. DOI PubMed
89. Zhu C, Lee SC, Chen H, Yue H, Rueping M. Reductive cross-coupling of α-oxy halides enabled by thermal catalysis, photocatalysis, electrocatalysis, or mechanochemistry. *Angew Chem Int Ed Engl* 2022;61:e202204212. DOI PubMed
90. Day CS, Rentería-gómez Á, Ton SJ, Gogoi AR, Gutierrez O, Martin R. Elucidating electron-transfer events in polypyridine nickel complexes for reductive coupling reactions. *Nat Catal* 2023;6:244-53. DOI
91. Tang T, Hazra A, Min DS, et al. Interrogating the mechanistic features of Ni(I)-mediated aryl iodide oxidative addition using electroanalytical and statistical modeling techniques. *J Am Chem Soc* 2023;145:8689-99. DOI
92. Chen PP, Lucas EL, Greene MA, et al. A unified explanation for chemoselectivity and stereospecificity of Ni-catalyzed kumada and cross-electrophile coupling reactions of benzylic ethers: a combined computational and experimental study. *J Am Chem Soc* 2019;141:5835-55. DOI
93. Hewitt KA, Xie P, Thane TA, et al. Nickel-catalyzed domino cross-electrophile coupling dicarbofunctionalization reaction to afford vinylcyclopropanes. *ACS Catal* 2021;11:14369-80. DOI
94. Lucas EL, Hewitt KA, Chen PP, Castro AJ, Hong X, Jarvo ER. Engaging sulfonamides: intramolecular cross-electrophile coupling reaction of sulfonamides with alkyl chlorides. *J Org Chem* 2020;85:1775-93. DOI PubMed
95. Xu Z, Yang Y, Jiang J, Fu Y. Theoretical investigation on Ni-catalyzed C(sp^3)-F activation and ring contraction of tetrahydropyrans: exploration of an S_N2 pathway. *Organometallics* 2018;37:1114-22. DOI
96. Lucas EL, Mcginnis TM, Castro AJ, Jarvo ER. Nickel-catalyzed cross-electrophile coupling of the difluoromethyl group for fluorinated cyclopropane synthesis. *Synlett* 2021;32:1525-30. DOI
97. Sanford AB, Thane TA, McGinnis TM, Chen PP, Hong X, Jarvo ER. Nickel-catalyzed alkyl-alkyl cross-electrophile coupling reaction of 1,3-dimesylates for the synthesis of alkylcyclopropanes. *J Am Chem Soc* 2020;142:5017-23. DOI PubMed PMC